

# High temperature electron spin relaxation in bulk GaAs

S. Oertel,<sup>a)</sup> J. Hübner, and M. Oestreich

Institute for Solid State Physics, Leibniz University Hannover, Appelstr. 2, 30167 Hannover, Germany

(Received 7 August 2008; accepted 10 September 2008; published online 1 October 2008)

Temperature and electron density dependent measurements of the electron spin relaxation in bulk GaAs are performed using time- and polarization-resolved photoluminescence spectroscopy. The electron spin relaxation time is dominated in the high temperature regime by the D'yakonov-Perel' [M. I. D'yakonov and V. I. Perel', Sov. Phys. Solid State **13**, 3023 (1972)] spin relaxation mechanism and decreases for negligible electron densities from 42 ps at 300 K to 20 ps at 400 K. The measured spin relaxation times are compared with numerical calculations which include electron-phonon momentum scattering and have no adjustable parameters. © 2008 American Institute of Physics. [DOI: 10.1063/1.2993344]

Spin relaxation in semiconductors is of fundamental importance for prospective spintronic devices.<sup>1-3</sup> At the same time, spin relaxation is an intriguing physics problem due to the complex interplay of fundamentally different processes leading to spin relaxation. Most of them play dominant roles in the well investigated semiconductor material GaAs and their efficiencies depend strongly on such various parameters like the electron energy and temperature, doping density, electron-hole overlap, electron-electron, electron-impurity, and electron-phonon scattering. The major four spin relaxation processes in bulk GaAs take place via hyperfine interaction,<sup>4,5</sup> the Elliott and Yafet,<sup>6</sup> the Bir-Aranov-Pikus,<sup>7</sup> and the D'yakonov-Perel' (DP) mechanisms. At low temperatures they can be of comparable magnitude and the identification of a dominant spin relaxation mechanism is accordingly difficult. However, in the technologically more interesting temperature regime at room temperature and above, the spin relaxation in bulk GaAs is unambiguously dominated by the DP mechanism.<sup>8</sup> Here, the electron momentum relaxation time  $\tau_p$  strongly affects the electron spin relaxation time  $\tau_s$  and is dominated at low carrier densities solely by interaction with longitudinal optical (LO) phonons and thus can be easily calculated analytically. Spin relaxation measurements at very high temperature are, hence, the ideal candidate for a *quantitative* comparison with spin relaxation theory.

In the first part of the paper the spin relaxation measurements on undoped bulk GaAs are presented followed by a comparison of the results with existing theory. The MBE grown sample consists of 5  $\mu\text{m}$  GaAs, which is separated from the substrate by a 2  $\mu\text{m}$  thick undoped  $\text{Al}_{0.3}\text{Ga}_{0.7}\text{As}$  layer.<sup>9</sup> Spin oriented electrons are optically injected by excitation with circularly polarized 100 fs laser pulses from a mode locked 80 MHz Ti:sapphire laser. The excitation energy of 1.59 eV is for all temperatures well below the valence splitoff to conduction band transition ensuring an initial electron spin polarization of about 50%.<sup>10,11</sup> During the very first picosecond after excitation, the carrier momentum distribution thermalizes by interaction with the phonon bath. During the same time the holes lose their spin orientation due to the strong valence band mixing and  $k$ -dependent spin splitting. The polarized photoluminescence (PL) is measured in backward direction and temporally resolved by a synchro-

scan streak camera with a time resolution of 6 ps. The two circular polarizations of the PL are sequentially detected by a switchable liquid crystal retarder and a polarizer in front of the streak camera. Figure 1(a) shows as example the temporal dynamics of both circular PL components and the resulting degree of polarization  $P$ . The PL lifetime is for all temperatures and carrier densities about 250 ps, i.e., the carrier density does not change significantly on the timescale of  $\tau_s$ . Also carrier diffusion can be neglected since bipolar carrier diffusion is slow compared to  $\tau_s$ .<sup>12</sup> The measured  $P$  of the PL, i.e., the electron spin polarization, can be well fitted by a monoexponential decay,<sup>13</sup> whereat the fit starts about 10 ps after excitation. Within these 10 ps the carriers thermalize with the lattice for all studied excitation densities by Fröhlich

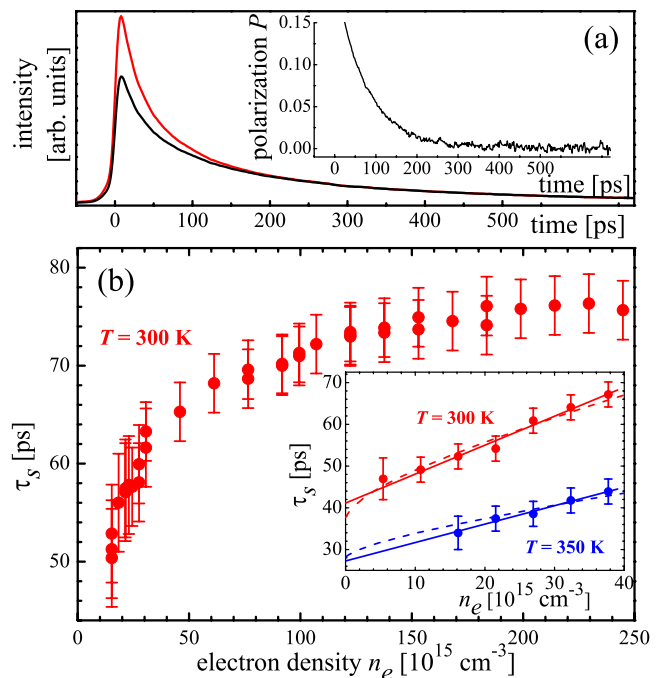


FIG. 1. (Color online) (a) Time resolved right and left circular polarized components of the PL at 300 K and an excitation density of  $1.2 \cdot 10^{17} \text{ cm}^{-3}$ . The inset shows the corresponding degree of polarization  $P$ . (b) Spin relaxation time  $\tau_s$  versus electron density  $n_e$  measured at 300 K. The inset shows the spin relaxation time in the low electron density regime for another data set. The linear density gradients are  $6.8 \times 10^{-16} \text{ ps cm}^3$  and  $4.4 \times 10^{-16} \text{ ps cm}^3$  for 300 and 350 K, respectively. The two dashed lines show accurate density dependence calculations beyond the motional narrowing regime.

<sup>a)</sup>Electronic mail: oertel@nano-uni.hannover.de.

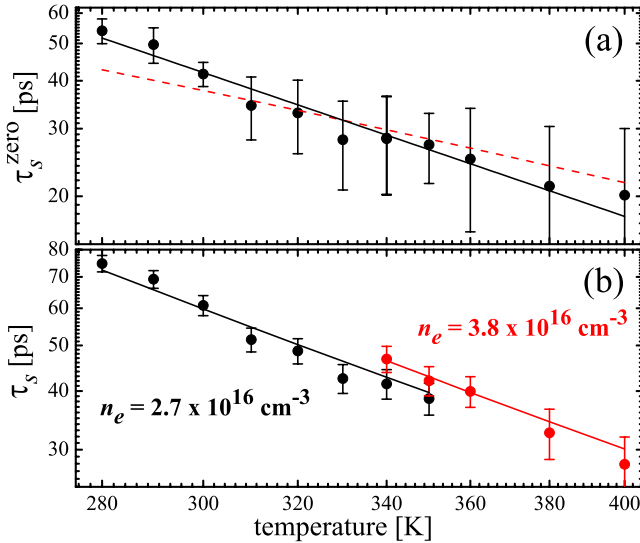


FIG. 2. (Color online) (a) Measured spin-relaxation time linearly extrapolated to zero electron density  $\tau_s^{\text{zero}}$  (double logarithmic scale). The solid line is a fit to the experimental data proportional to  $T^{-3}$ . The dashed, red line is a numerical *quantitative* calculation according to Eq. (4). (b) Raw experimental  $\tau_s$  (dots) and calculated  $\tau_s$  (solid lines) at finite densities.

interaction, which is extremely efficient at high temperatures.<sup>14</sup>

Figure 1(b) depicts the measured  $\tau_s$  at room temperature in dependence on carrier density. At low densities,  $\tau_s$  increases in the regime from  $5 \times 10^{15}$  to  $2.5 \times 10^{17} \text{ cm}^{-3}$  linearly with carrier density. Such a linear dependence was predicted in the motional narrowing regime by Glazov and Ivchenko,<sup>15</sup> who calculated a linear dependence of the electron-electron scattering rate  $\Gamma_p^{ee}$  on the electron density  $n_e$  in the quasielastic scattering limit, i.e.,  $\Gamma_p^{ee} \propto n_e \Rightarrow \tau_s^{ee} \propto n_e$ . The theory also predicts a reduction in  $\Gamma_p^{ee}$  with increasing temperature, which results in a reduced density dependence of  $\tau_s$  with increasing temperature as is confirmed experimentally [inset of Fig. 1(b)]. At high carrier densities the measured  $\tau_s$  becomes nearly independent on  $n_e$  with  $\tau_s \approx 75 \text{ ps}$  for densities of  $10^{17} \text{ cm}^{-3}$ , which compares well with comparable measurements.<sup>10,16,17</sup> We further checked that  $\tau_s$  shows within our measurement accuracy no dependence on the degree of the electron spin polarization at these carrier densities. Two reasons are responsible for the saturation of  $\tau_s$  at high densities: as an intrinsic effect enhanced screening of the electron-electron interaction and phase space filling reduces the increase in the electron-electron scattering probability with increasing density. Furthermore, local heating of the lattice by the laser pulses reduces  $\tau_s$ .

Next, we study the temperature dependence of  $\tau_s$ . The measurements have been carried out at a fixed electron density of  $2.7 \times 10^{16} \text{ cm}^{-3}$  for temperatures between 280 and 340 K and  $3.8 \times 10^{16} \text{ cm}^{-3}$  between 360 and 400 K. The raised excitation density compensates for the decreasing signal to noise ratio, which results from the decrease in PL intensity with increasing temperature.<sup>18</sup> Using the measured density gradients of  $\tau_s$  at 300 and 350 K from the inset of Fig. 1(b) we interpolate the density gradient for all temperatures and extrapolate from the measurements at finite density the intrinsic spin lifetime at zero density  $\tau_s^{\text{zero}}$  in the entire temperature regime as shown in Fig. 2(a).

Below, a qualitative and quantitative description of the data follows. The DP mechanism is based on the  $k$ -dependent

spin splitting of the conduction band for  $k \neq 0$ . The spin splitting can be described by an effective magnetic field  $\vec{B}(\vec{k})$  around which each individual electron spin precesses with its own Larmor frequency  $\vec{\Omega}(\vec{k})$ . Since  $\vec{\Omega}$  depends on  $\vec{k}$ , electron momentum scattering changes  $\vec{\Omega}$  and, hence, leads to spin dephasing. In the special case of  $\Omega \tilde{\tau}_p \gg 1$ , the resulting spin relaxation time  $\tilde{\tau}_s$  is about equal to the momentum relaxation time  $\tilde{\tau}_p$ .<sup>1</sup> Here and in the following a tilde denotes an entity at a given energy. In the more usual case of  $\Omega \tilde{\tau}_p \ll 1$ , the energy dependent DP spin relaxation rate in the motional narrowing regime  $1/\tilde{\tau}_s'$  is given by<sup>1,10</sup>

$$\frac{1}{\tilde{\tau}_s'} = \frac{32}{105} \alpha_c^2 \frac{E_k^3}{\hbar^2 E_g} \left( \sum_i \frac{\gamma_i^j}{\tilde{\tau}_p^j} \right)^{-1}, \quad (1)$$

where  $\alpha_c = 0.063$  is the spin splitting parameter of the conduction band corresponding to a Dresselhaus splitting of  $\gamma_c = 21.9 \text{ eV \AA}^3$ . The electron excess energy is denoted by  $E_k$  and  $E_g$  is the band-gap energy. The energy dependent scattering rates  $1/\tilde{\tau}_p^j$  for the different momentum scattering processes are added up in Eq. (1) with corresponding efficiency factors  $\gamma_i^j$  (for polar-optical phonon scattering  $\gamma_3^{\text{POP}} = 11/6$ ),<sup>19</sup> that express how effective the related scattering mechanism changes  $\vec{\Omega}$ .<sup>20</sup> The physical relevant spin relaxation rate  $\Gamma_s$  of the whole electron ensemble is given in the regime of motional narrowing by averaging  $1/\tilde{\tau}_s'$  over all energies.

Pikus and Titkov<sup>10</sup> calculated  $\Gamma_s$  for the case of a non-degenerate electron gas and an averaged momentum relaxation time  $\tau_p^j$  by thermally averaging Eq. (1) over the Boltzmann distribution:

$$\frac{1}{\tau_s^j} = Q^j \tau_p^j \alpha_c^2 \frac{(k_B T)^3}{\hbar^2 E_g}, \quad (2)$$

where  $Q^j$  is a numerical factor depending on the corresponding momentum scattering mechanism. In the case of polar-optical phonon (POP) scattering  $Q^{\text{POP}} = 3$ .<sup>19</sup> Qualitatively, Eq. (2) describes the  $T^{-3}$  dependence of the experimental data well [see solid line in Fig. 2(a)]. Quantitatively, Eq. (2) differs from the experimental data approximately by a factor of 4 if we use for the calculation an average momentum scattering time  $\tau_p = 280 \text{ fs}$  at 300 K obtained from mobility measurements.<sup>21</sup> Such difference by a factor of 4 is not surprising since Eq. (2) contains some significant simplifications.<sup>22</sup>

Last, we calculate  $\tau_s$  for a quantitative comparison. Equation (1) is valid in the motional narrowing regime  $\Omega \tilde{\tau}_p \ll 1$ , i.e., for low electron energies. For high electron energies  $\Omega \tilde{\tau}_p \gg 1$ , the energy dependent spin relaxation rate results from the energy dependent Larmor frequency averaged over all  $k$ -directions. Combining both regimes, the spin relaxation rate for all electron energies can be approximated by<sup>23</sup>

$$\frac{1}{\tilde{\tau}_s} = \left( \frac{1}{\tilde{\tau}_s'} + \frac{\hbar \sqrt{128 E_g}}{\alpha_c E_k^{3/2}} \right)^{-1}. \quad (3)$$

Integrating over all energies then yields

$$\frac{1}{\tau_s} = \frac{\int_0^\infty (\tilde{\tau}_s)^{-1} f(E_k) D(E_k) dE_k}{\int_0^\infty f(E_k) D(E_k) dE_k}, \quad (4)$$

where  $f(E_k)$  is the Fermi distribution and  $D(E_k) \propto \sqrt{E_k}$  is the three-dimensional density of states. The energy dependent momentum relaxation rate is calculated by an analytic equation derived by Callen<sup>24</sup> and later by Ridley<sup>25</sup> for POP scattering [see Eq. (5)] where  $\hbar\omega_{LO}$  is the polar-optical phonon energy,  $\epsilon_\infty$  and  $\epsilon$  are the high and low frequency dielectric constants,  $m$  is the effective electron mass, and  $n(\omega_{LO}) = \exp(\frac{\hbar\omega_{LO}}{k_B T} - 1)^{-1}$ . Accounting for POP scattering only is a very good approximation since piezoelectric and deformation potential scattering by acoustic phonons and ionized impurity scattering at low doping concentrations are according to our calculations insignificant compared to POP scattering.

$$\begin{aligned} \frac{1}{\tilde{\tau}_p^{\text{POP}}} = & \frac{e^2 \omega_{LO} m^{1/2}}{2^{5/2} \pi \hbar (\epsilon_\infty^{-1} - \epsilon^{-1})^{-1} \epsilon_0 E_k^{1/2}} \times \left( n(\omega_{LO}) \right. \\ & \times \left[ \sqrt{1 + \frac{\hbar\omega_{LO}}{E_k}} - \frac{\hbar\omega_{LO}}{E_k} \sinh^{-1} \sqrt{\frac{E_k}{\hbar\omega_{LO}}} \right] \\ & + \{n(\omega_{LO}) + 1\} \left[ \sqrt{1 - \frac{\hbar\omega_{LO}}{E_k}} \right. \\ & \left. \left. + \frac{\hbar\omega_{LO}}{E_k} \sinh^{-1} \sqrt{\frac{E_k}{\hbar\omega_{LO}} - 1} \right]_{E_k > \hbar\omega_{LO}} \right). \quad (5) \end{aligned}$$

The dashed line of Fig. 2(a) depicts the resulting  $\tau_s^{\text{zero}}$  calculated without adjustable parameter. The slope of the calculated  $\tau_s^{\text{zero}}$  is weaker than the  $T^{-3}$  dependence in Eq. (2) since electron momentum scattering by POP is more efficient at higher temperatures. Nevertheless, the noncomplex calculations are in astonishingly good *quantitative* agreement with the measurements. The discrepancies at high as well as for the lower temperatures are well within the error bars and the uncertainties of the density dependent measurements [see inset of Fig. 1(b)]. Furthermore the impact of other momentum scattering mechanisms increases with decreasing temperature, i.e., in the calculations additional scattering mechanisms must be included at low temperatures, which on the other hand increases the number of uncertainties and relaxes the explanatory power of the shown equations.

We want to point out that the linear extrapolation of  $\tau_s$  to zero density [inset of Fig. 1(b)] is a good approximation but strictly valid only in the pure motional narrowing regime. Therefore, we have additionally calculated  $\tau_s$  at finite carrier densities by including in Eq. (1) an energy dependent electron-electron scattering time<sup>15</sup>  $\tilde{\tau}_p^{ee} \propto E_k^{3/2}$  by  $\gamma_3^{ee}/\tilde{\tau}_p^{ee} = C^{-1} n_e E_k^{-3/2}$ , where  $C$  is a constant. We have determined  $C = 1.5 \times 10^5 \text{ eV}^{-3/2} \text{ cm}^{-3} \text{ s}$  experimentally by fitting the calculations to the measured density dependence of  $\tau_s$  at 300 K [experimental data of the inset of Fig. 1(b); the dashed line shows the fit]. The same  $C$  describes the density dependence of  $\tau_s$  at 350 K with high accuracy and yields at 300 K and  $n_e = 10^{17} \text{ cm}^{-3}$  an energy averaged, effective electron-electron scattering rate  $\gamma_3^{ee}/\tilde{\tau}_p^{ee} = 7.2 \times 10^{13} \text{ s}^{-1}$ , which is in very good agreement with other, independent experiments.<sup>26</sup> Our calculations show that the deviation between the calculated and the linear extrapolated density dependence becomes more extensive at low electron densities and with decreasing temperature. Figures 2(a) and 2(b) clarify this

deviation, whereat Fig. 2(b) depicts the calculated (straight lines) and the measured temperature dependence of  $\tau_s$  (dots) at finite densities and shows an excellent agreement of both.

In conclusion, we have measured the electron spin relaxation time in bulk GaAs in the high temperature regime using time- and polarization-resolved PL spectroscopy. The dependence of the spin relaxation time on electron density is investigated at 300 and 350 K by high accuracy measurements and used to extrapolate  $\tau_s$  between 280 and 400 K to zero electron density. The measured intrinsic spin relaxation times are in excellent *quantitative* agreement with calculations using solely D'yakonov-Perel' spin relaxation and electron polar-optical phonon scattering.

We thank Michael Krauss for valuable discussions and Markus Beck for providing the sample. This work has been supported by the DFG and the BMBF (NanoQuit).

- <sup>1</sup>I. Žutić, J. Fabian, and S. Das Sarma, *Rev. Mod. Phys.* **76**, 323 (2004).
- <sup>2</sup>M. Oestreich, M. Bender, J. Hübner, D. Hägele, W. W. Rühle, T. Hartmann, P. J. Klar, W. Heimbrodt, M. Lampalzer, K. Volz, and W. Stolz, *Semicond. Sci. Technol.* **17**, 285 (2002).
- <sup>3</sup>J. Rudolph, D. Hägele, H. M. Gibbs, G. Khitrova, and M. Oestreich, *Appl. Phys. Lett.* **82**, 4516 (2003); J. Rudolph, S. Döhrmann, D. Hägele, M. Oestreich, and W. Stolz, *ibid.* **87**, 241117 (2005).
- <sup>4</sup>G. Fishman and G. Lampel, *Phys. Rev. B* **16**, 820 (1977).
- <sup>5</sup>D. Paget, *Phys. Rev. B* **24**, 3776 (1981).
- <sup>6</sup>R. J. Elliott, *Phys. Rev.* **96**, 266 (1954); Y. Yafet, *Solid State Physics* (Academic, New York, 1963), Vol. 14.
- <sup>7</sup>G. L. Bir, A. G. Aronov, and G. E. Pikus, *Sov. Phys. JETP* **42**, 705 (1976).
- <sup>8</sup>P. H. Song and K. W. Kim, *Phys. Rev. B* **66**, 035207 (2002).
- <sup>9</sup>A present, compared to the excitation density, low n-type background doping of  $1.2 \cdot 10^{15} \text{ cm}^{-3}$  of the GaAs yields no appreciable electron-impurity scattering and is therefore negligible for this experiment. Furthermore, the structure is covered by a thin, highly n-doped GaAs cap layer to adjust the Fermi level at the surface.
- <sup>10</sup>G. E. Pikus and A. N. Titkov, *Optical Orientation* (North-Holland, Amsterdam, 1984), Vol. 8.
- <sup>11</sup>S. Pfalz, R. Winkler, T. Nowitzki, D. Reuter, A. D. Wieck, D. Hägele, and M. Oestreich, *Phys. Rev. B* **71**, 165305 (2005).
- <sup>12</sup>A. Miller, R. J. Manning, P. K. Milsom, D. C. Hutchings, D. W. Crust, and K. Woodbridge, *J. Opt. Soc. Am. B* **6**, 567 (1989).
- <sup>13</sup>All measured  $P$  are well fitted by a monoexponential decay, which confirms that carrier density and carrier and lattice temperature do not change significantly on the timescale of  $\tau_s$ .
- <sup>14</sup>K. Leo, W. W. Rühle, H. J. Queisser, and K. Ploog, *Phys. Rev. B* **37**, 7121 (1988).
- <sup>15</sup>M. M. Glazov and E. L. Ivchenko, *Sov. Phys. JETP* **99**, 1279 (2004).
- <sup>16</sup>P. E. Hohage, G. Bacher, D. Reuter, and A. D. Wieck, *Appl. Phys. Lett.* **89**, 231101 (2006).
- <sup>17</sup>R. S. Britton, T. Grevatt, A. Malinowski, R. T. Harley, P. Perozzo, A. R. Cameron, and A. Miller, *Appl. Phys. Lett.* **73**, 2140 (1998).
- <sup>18</sup>The 40% increase in the excitation density at high temperatures is unproblematic since electron screening and phase space filling effects are less pronounced at higher temperatures.
- <sup>19</sup>The correct values of  $\gamma_3^{\text{POP}}$  and  $Q^{\text{POP}}$  are given in the Russian version of Ref. 10.
- <sup>20</sup>J. Fabian, A. Matos-Abiague, C. Ertler, P. Stano, and I. Zutic, *Acta Phys. Slov.* **57**, 565 (2007).
- <sup>21</sup>G. E. Stillman, C. M. Wolfe, and J. O. Dimmock, *J. Phys. Chem. Solids* **31**, 1199 (1970).
- <sup>22</sup>A. Dyson and B. K. Ridley, *Phys. Rev. B* **69**, 125211 (2004).
- <sup>23</sup>M. Beck, *Electron Spin Relaxation, Transport and Strain-Induced Precession in n-GaAs* (Lehrstuhl für Mikrocharakterisierung, Friedrich-Alexander-Universität, Erlangen Nürnberg, Erlangen, 2005).
- <sup>24</sup>H. B. Callen, *Phys. Rev.* **76**, 1394 (1949).
- <sup>25</sup>B. K. Ridley, *Quantum Processes in Semiconductors* (Oxford University Press, New York, 1988).
- <sup>26</sup>M. T. Portella, J.-Y. Bigot, R. W. Schoenlein, J. E. Cunningham, and C. V. Shank, *Appl. Phys. Lett.* **60**, 2123 (1992).